Electronic Entropy, Shell Structure, and Size-Evolutionary Patterns of Metal Clusters

Constantine Yannouleas and Uzi Landman

School of Physics, Georgia Institute of Technology, Atlanta, Georgia 30332-0430

We show that electronic-entropy effects in the size-evolutionary patterns of relatively small (as small as 20 atoms), simple-metal clusters already become prominent at moderate temperatures. Detailed agreement between our finite-temperature–shell-correction-method calculations and experimental results is obtained for certain temperatures. This agreement includes a size-dependent smearing out of fine-structure features, accompanied by a measurable reduction of the heights of the steps marking major-shell and subshell closings, thus allowing for a quantitative analysis of cluster temperatures. [S0031-9007(97)02448-4]

Since the discovery [1] of electronic-shell-structure features in the abundance spectra of sodium clusters, similar features (the major ones corresponding to the degeneracies of a spherically symmetric mean-field potential [2,3]) have been routinely observed [4] in the size-evolutionary patterns (SEP's) associated with other single-particle properties of both alkali- and noble-metal clusters. Specifically, such patterns pertain to ionization potentials (IP's) [5–7], electron affinities (EA's) [8,9], monomer separation energies (MSE's) [10], and fission dissociation energies [11].

It was early realized [12] that the secondary features in the mass spectra required the consideration of deformed cluster shapes [5,12]. When triaxial (ellipsoidal) shapes were considered in the framework of shell correction methods (SCM) [13–16], substantial overall systematic agreement was achieved [14,15] between theory and experimental observations pertaining to the major and the fine structure of the aforementioned SEP's.

While deformation effects have been extensively studied, an understanding of the physical origins of thermal effects and their relation to the SEP's is still lacking, even though the experiments are necessarily made with clusters at finite temperatures. Moreover, experimental determination of cluster temperatures remains a challenge, motivating the development of theoretical methods capable of extracting such information.

While thermodynamic entropic contributions associated with the ionic degrees of freedom can be obtained from first-principles molecular-dynamics simulations [17,18], or from considerations of shape fluctuations in simpler models [19–21], for sufficiently large simple-metal clusters M_N with $N > 20$, the electronic entropy (which has not as yet been included in such studies) dominates the thermal characteristics of the shell structure, even at moderate temperatures. The prominent thermal effects associated with the electronic entropy are the focus of this paper.

Without the simultaneous consideration of shape fluctuations, thermal effects pertaining to the electronic degrees of freedom and their relevance for the understanding of mass abundance spectra have been considered in the case of spherical neutral sodium clusters [22], and in a recent report [23] on the thermodynamics of neutral sodium clusters with axially symmetric shapes. In contrast to our findings, these studies have suggested that electronic-entropy effects at moderate temperatures are not important for clusters with less than 100 atoms.

The theoretical method used in this paper is a finite-temperature (FT) -SCM developed by us, which incorporates all three of the aforementioned aspects, namely, triaxial deformations, entropy of the electrons, and thermal effects originating from shape fluctuations. Furthermore, through a direct comparison with experimental measurements, we demonstrate that this method can be employed for determining cluster temperatures.

Since the number of delocalized valence electrons is fixed for a given cluster, $M_N^{x\pm}$, we need to use [24,25] the *canonical* ensemble in calculating their thermodynamical properties. For determining the free energy, $F(\beta, N, x)$ ($\beta = 1/T$), which incorporates the electronic entropy, we separate it, in analogy with the zero-temperature limit [14], into a smooth, liquid-drop-model (LDM) part, $\tilde{F}_{\mathrm{LDM}}$, and a Strutinsky-type [26] shell-correction term, ΔF_{sh}. The shell correction term is specified as the difference $\Delta F_{\mathrm{sh}} = F_{\mathrm{sp}} - \tilde{F}_{\mathrm{sp}}$, where F_{sp} is the canonical free energy of the valence electrons viewed as independent single particles in their effective mean-field potential. For calculating the canonical F_{sp}, we adopt a number-projection method [27], according to which

$$F_{\mathrm{sp}} = -\frac{1}{\beta} \ln\left(\int_0^{2\pi} \frac{d\phi}{2\pi} Z_{\mathrm{GC}}(\beta, \beta\mu + i\phi) \right.$$
$$\left. \times\, e^{-(\beta\mu + i\phi)N_e} \right),$$

where N_e is the number of electrons and μ is the chemical potential of the equivalent grand-canonical ensemble. The grand-canonical partition function, Z_{GC}, is given by

$$Z_{\mathrm{GC}}(\beta, \beta\mu) = \prod_i (1 + e^{-\beta(\varepsilon_i - \mu)}),$$

where ε_i are the single-particle levels of the modified Nilsson Hamiltonian pertaining to triaxial shapes [14].

The temperature-dependent average $\widetilde{F}_{\rm sp}$ [28] is specified using the same expressions as for $\widetilde{F}_{\rm sp}$, but with a set of smooth levels [23] defined as $\widetilde{\varepsilon}_i = \widetilde{E}_{\rm sp}^{\rm osc}(i) - \widetilde{E}_{\rm sp}^{\rm osc}(i-1)$, where $\widetilde{E}_{\rm sp}^{\rm osc}(N_e)$ is the zero-temperature Strutinsky average of the single-particle spectrum of an anisotropic, triaxial oscillator (see Section II.C. of Ref. [14]).

The LDM term $\widetilde{F}_{\rm LDM}$ consists of three contributions; a volume, a surface, and a curvature term. Since volume conservation during deformation is assumed, we need not consider the temperature dependence of the corresponding term when calculating observables, such as IP's and MSE's, associated with processes which do not change the total number of atoms, N. The experimental temperature dependence of the surface tension, $\sigma(T) = c_0 - c_1(T - T_{\rm mp})$, is taken from standard tables [29] ($T_{\rm mp}$ are melting-point temperatures [30]), but normalized to yield the $\sigma(T = 0)$ value used in our earlier calculations [14]. Since no experimental information is available regarding the curvature coefficient, A_c, we assume the same relative temperature dependence as for $\sigma(T)$ normalized to the $T = 0$ value used earlier [14]. Finally, the expansion of the Wigner-Seitz radius due to the temperature is determined according to the coefficient of linear thermal expansion [30]. With these modifications, the remaining steps in the calculation of $\widetilde{F}_{\rm LDM}$ follow closely Section II.A. of Ref. [14] (for simplicity, the work function W is assumed temperature independent).

According to the general theory of thermal fluctuating phenomena [31], the triaxial shapes of the clusters, specified by the β_H and γ_H Hill-Wheeler parameters [32], will explore [33] the free-energy surface, $F(\beta, N, x; \beta_H, \gamma_H)$, with a probability,

$$P(\beta_H, \gamma_H) = Z^{-1} \exp[-\beta F(\beta, N, x; \beta_H, \gamma_H)],$$

the quantity Z being the classical Boltzmann-type partition function,

$$Z = \int d\tau \exp[-\beta F(\beta, N, x; \beta_H, \gamma_H)],$$

and $d\tau = \beta_H^4 |\sin(3\gamma_H)| d\beta_H d\gamma_H$ the proper volume element [34]. Thus, finally, the free energy, $\langle F(\beta, N, x)\rangle$, averaged over the shape fluctuations can be written as

$$\langle F(\beta, N, x)\rangle = \int d\tau F(\beta, N, x; \beta_H, \gamma_H)$$
$$\times P(\beta_H, \gamma_H).$$

We will present results pertaining to IP's and MSE's ($M_N^+ \to M_{N-1}^+ + M$), which at finite temperatures are defined as

$$I_N = \langle F(\beta, N, x = +1)\rangle - \langle F(\beta, N, x = 0)\rangle$$

and

$$D_{1,N}^+ = \langle F(\beta, N-1, x = +1)\rangle + \langle F(\beta, N = 1, x = 0)\rangle$$
$$- \langle F(\beta, N, x = +1)\rangle,$$

respectively.

Our calculations (solid dots) for the IP's of K_N clusters for three temperatures, $T = 10$, 300, and 500 K, are displayed in Fig. 1, and are compared with the experimental measurements [5] (open squares; the experimental uncertainties are 0.06 eV for $N \le 30$ and 0.03 eV for $N > 30$). As was the case with our earlier $T = 0$ K results [14], the $T = 10$ K theoretical results exhibit the following two characteristics: (i) above $N = 21$, a pronounced fine structure between major-shell closures which is not present in the experimental measurements; (ii) steps at the major-shell closures which are much larger than the experimental ones [35] (3 to 5 times for $N = 40$, 58, and 92, and 2 to 3 times for $N = 8$ and 20).

The agreement between theory and experiment is significantly improved at $T = 300$ K. Indeed, in comparison with the lower-temperature calculations, the $T = 300$ K results exhibit the following remarkable changes: (i) Above $N = 21$, the previously sharp fine-structure features are smeared out, and as a result, the theoretical curve follows closely the smooth modulations of the experimental profile. In the size range $N = 21$–34, three rounded, humplike formations (ending to the right at the subshell closures at $N = 26$, 30, and 34) survive in very good agreement with the experiment (the sizes of the drops at $N = 26$, 30, and 34 are comparable to the experimental ones [36]). (ii) The sizes of the IP drops at $N = 20$, 40, 58, and 92 are reduced drastically and are now comparable to the experimental ones. In the size range $N \le 20$,
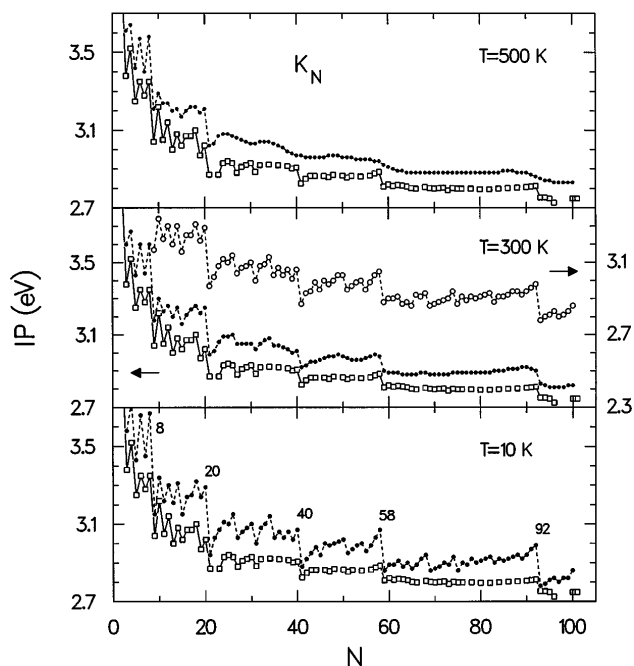
FIG. 1. IP's of K_N clusters at three temperatures, $T = 10$, 300, and 500 K. Solid dots: theoretical FT-SCM results. Open squares: experimental measurements [5]. The uppermost curve (open circles) in the middle panel displays theoretical results when the electronic entropy is neglected. The y scale in this instance is to the right.

the modifications are not as dramatic. Indeed, one can clearly see that the pattern of odd-even alternations remains well defined, but with a moderate attenuation in amplitude, again in excellent agreement with the experimental observation.

For $T = 500$ K, the smearing out of the shell structure progresses even further, obliterating the agreement between theory and experiment. Specifically, the steps at the subshell closures at $N = 26$ and 30, as well as at the major-shell closures at $N = 40$, 58, and 92, are rounded and smeared out over several clusters (an analogous behavior has been observed in the logarithmic abundance spectra of hot, singly cationic, copper, silver, and gold clusters [37]). At the same time, however, the odd-even alternation remains well defined for $N \leq 8$. We further notice that, while some residue of fine structure survives in the range $N = 9$–15, the odd-even alternations there are essentially absent (certain experimental measurements [38] of the IP's of hot Na$_N$ clusters appear to conform to this trend).

To ascertain the relative weight of the two thermal processes incorporated in our FT-SCM, we display in the middle panel of Fig. 1 (uppermost curve with open circles) the theoretical IP's at $T = 300$ K in the case when the electronic entropy is neglected. A comparison with the results (solid dots) when both electronic and shape-fluctuation entropic contributions are included demonstrates the principal role of the electronic entropy in shaping the thermal effects of the SEP's.

Figure 2 displays for two temperatures (10 and 300 K) the FT-SCM results (solid dots) for the MSE's associated with the K$_N^+$ clusters, along with the available experimental measurements [10] (open squares) in the size range $N = 4$–23. Compared to the $T = 10$ K results,
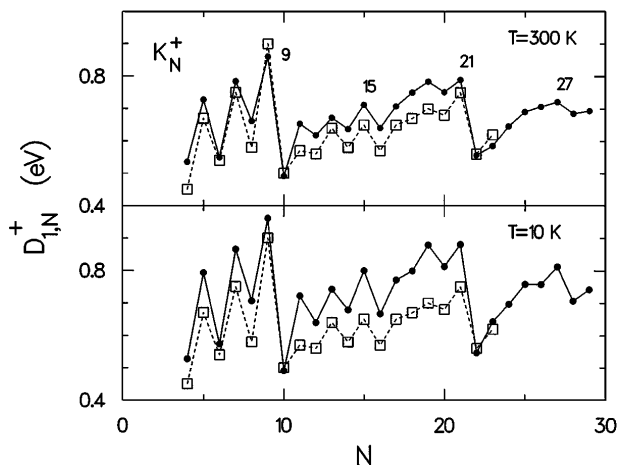
the theoretical results at $T = 300$ K are in better agreement with the experimental ones due to an attenuation of the amplitude of the alternations (e.g., notice the favorable reduction in the size of the drops at $N = 9$, 15, and 21). In spite of this amplitude attenuation, it is remarkable that the $T = 300$ K SCM results in this size range preserve in detail the same relative pattern as the $T = 10$ K ones (in particular, the well-defined odd-even oscillations in the range $N = 4$–15 and the ascending quartet at $N = 16$–19 followed by a dip at $N = 20$).

As a last example, Fig. 3 displays for three temperatures (10, 800, and 2000 K) our FT-SCM results for the IP's of Ag$_N$ clusters, and compares them with available experimental measurements [6,39]. Again, going from the $T = 10$ K to the $T = 800$ K results, we observe that an attenuation of the amplitude of alternations brings theory and experiment into better agreement (e.g., in the latter case, the sizes of the theoretical IP drops at $N = 6$, 8, 14, 20, 26, 30, and 34 are comparable to the experimental ones). Finally, at $T = 2000$ K, both major and fine structures tend to vanish for $N > 8$.

In conclusion, we showed that the SEP's of the single-particle properties of simple-metal clusters are governed by the interplay of ellipsoidal deformations and thermodynamics (entropy) of the electronic degrees of freedom, while the entropic contribution of shape fluctuations plays a smaller role [40]. We further demonstrated that electronic-entropy effects are reflected in prominent experimental signatures already at moderate temperatures and for relatively small sizes. This behavior, which had

FIG. 2. MSE's of K$_N^+$ clusters at two temperatures, $T = 10$ and 300 K. Solid dots: Theoretical FT-SCM results. Open squares: experimental measurements [10]. To facilitate comparison, the SCM results at the higher temperature have been shifted by 0.07 eV, so that the theoretical curves at both temperatures refer to the same point at $N = 10$.
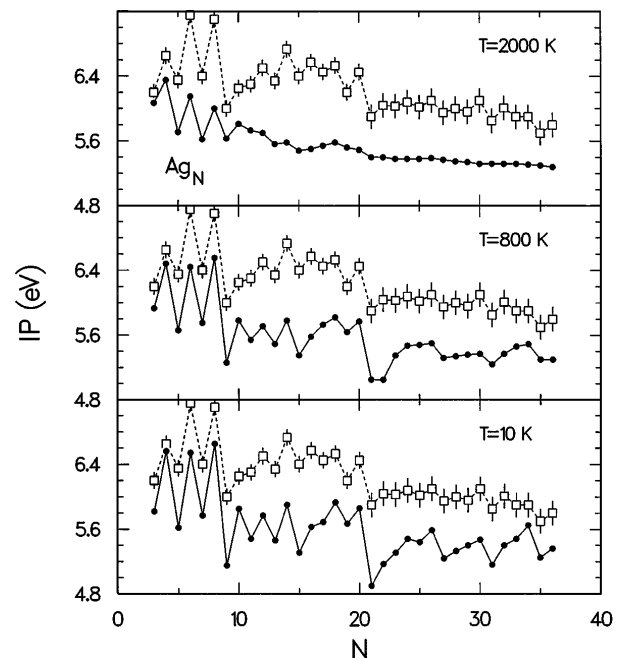
FIG. 3. IP's of Ag$_N$ clusters at three temperatures, $T = 10$, 800, and 2000 K. Solid dots: theoretical FT-SCM results. Open squares: experimental measurements [6].

not been previously understood in the case of metal clusters, correlates with an order-of-magnitude estimate [34] from theoretical nuclear physics. Accordingly, the shell-correction term in the free energy depends on T (here in energy units) as $\Delta F_{sh}(T) = \Delta F_{sh}(0)\tau/\sinh\tau$, which for $\tau > 1$ takes the form $2\Delta F_{sh}(0)\tau\exp(-\tau)$ with $\tau = 2\pi^2 T/(\hbar\omega_{sh})$, with $\hbar\omega_{sh}$ being the energy spacing between shells. Because of the large $2\pi^2$ factor, the shell-structure effects decrease rapidly, even for temperatures that are only a fraction of the shell spacing (see page 608 of Ref. [34]). Thus, the shell structure "melts" for temperatures as low as $T/(\hbar\omega_{sh}) = 0.25$ [41]. The FT-SCM calculations presented here correspond to temperature ranges well below this ratio, where analysis of the extent of attenuation of shell-structure signatures allows determination of cluster temperatures.

Compared to nuclear and atomic physics, which have heretofore provided the prototypes for fermionic shell structure, the SEP's of metal clusters stand apart, since the experimentally available SEP's of nuclei (e.g., those of neutron separation energies [42]) and of atoms (i.e., IP's [42]) correspond strictly to zero temperature. Finally, it is natural to conjecture that thermal (in particular, electronic-entropy) effects will influence the height of fission barriers and fragmentation channels [43].

[1] W. D. Knight *et al.,* Phys. Rev. Lett. **52**, 2141 (1984).

[2] W. Ekardt, Phys. Rev. B **29**, 1558 (1984).

[3] D. E. Beck, Solid State Commun. **49**, 381 (1984).

[4] W. A. de Heer, Rev. Mod. Phys. **65**, 611 (1993).

[5] W. A. Saunders, Ph.D. dissertation, University of California, Berkeley, 1986; W. A. Saunders *et al.,* Phys. Rev. B **32**, 1366 (1985).

[6] C. Jackschath *et al.,* Z. Phys. D **22**, 517 (1992).

[7] G. Alameddin *et al.,* Chem. Phys. Lett. **192**, 122 (1992).

[8] J. G. Eaton *et al.,* in *Nuclear Physics Concepts in the Study of Atomic Cluster Physics,* edited by R. Schmidt *et al.,* Lecture notes in Physics (Springer, Berlin, 1992), Vol. 404, p. 291.

[9] K. J. Taylor *et al.,* J. Chem. Phys. **96**, 3319 (1992).

[10] C. Bréchignac *et al.,* J. Chem. Phys. **93**, 7449 (1990).

[11] C. Bréchignac *et al.,* Phys. Rev. B **44**, 11 386 (1991).

[12] K. Clemenger, Phys. Rev. B **32**, 1359 (1985); Ph.D. dissertation, University of California, Berkeley, 1985.

[13] C. Yannouleas and U. Landman, Phys. Rev. B **48**, 8376 (1993); Chem. Phys. Lett. **210**, 437 (1993).

[14] C. Yannouleas and U. Landman, Phys. Rev. B **51**, 1902 (1995).

[15] C. Yannouleas and U. Landman, in *Large Clusters of Atoms and Molecules,* edited by T. P. Martin, NATO Advanced Study Institutes, Series E, Vol. 313 (Kluwer, Dordrecht, 1996), p. 131.

[16] For an application of our SCM to metal-cluster fission, see C. Yannouleas and U. Landman, J. Phys. Chem. **99**, 14 577 (1995); C. Yannouleas *et al.,* Comments At. Mol. Phys. **31**, 445 (1995). For an application to multiply charged fullerenes, see C. Yannouleas and U. Landman, Chem. Phys. Lett. **217**, 175 (1994), and to ^{3}He clusters see C. Yannouleas and U. Landman, J. Chem. Phys. **105**, 8734 (1996); Phys. Rev. B **54**, 7690 (1996).

[17] U. Röthlisberger and W. Andreoni, J. Chem. Phys. **94**, 8129 (1991).

[18] R. N. Barnett *et al.,* Phys. Rev. Lett. **67**, 3058 (1991).

[19] V. M. Akulin *et al.,* Phys. Rev. Lett. **75**, 220 (1995).

[20] M. Manninen *et al.,* Z. Phys. D **31**, 259 (1994).

[21] I.e., random-matrix (see Ref. [19]), independent-particle, and Hückel (see Ref. [20]) models in conjunction with a zero-temperature electron gas.

[22] M. Brack, Rev. Mod. Phys. **65**, 677 (1993).

[23] S. Frauendorf and V. V. Pashkevich, in Ref. [15], p. 201.

[24] R. Denton *et al.,* Phys. Rev. B **7**, 3589 (1973).

[25] R. Kubo, J. Phys. Soc. Jpn. **17**, 975 (1962).

[26] V. M. Strutinsky, Nucl. Phys. **A95**, 420 (1967).

[27] R. Rossignoli, Phys. Rev. C **51**, 1772 (1995).

[28] A. S. Jensen and J. Damgaard, Nucl. Phys. **A203**, 578 (1973).

[29] *Handbook of Chemistry and Physics,* edited by R. C. Weast (CRC Press, Cleveland, 1974), p. F-23.

[30] J. Emsley, *The Elements* (Oxford University Press, New York, 1991).

[31] L. D. Landau and E. M. Lifshitz, *Statistical Physics* (Pergamon, Oxford, 1980), Part 1, Chap. XII.

[32] D. L. Hill and J. A. Wheeler, Phys. Rev. **89**, 1102 (1953).

[33] C. Yannouleas *et al.,* Phys. Rev. B **41**, 6088 (1990); J. M. Pacheco *et al.,* Phys. Rev. Lett. **61**, 294 (1988).

[34] Å. Bohr and B. R. Mottelson, *Nuclear Structure* (Benjamin, Reading, MA, 1975), Vol. II.

[35] In contrast, experimental IP's for cold Na_N clusters are in good overall agreement with our $T = 0$ K SCM results regarding both characteristics (see Refs. [14,15]).

[36] Notice that experimental measurements at $N = 33$ and 35 have not been obtained (see Ref. [5]).

[37] I. Katakuse *et al.,* Int. J. Mass. Spectrom. Ion Process. **67**, 229 (1985).

[38] M. M. Kappes *et al.,* Chem. Phys. Lett. **143**, 251 (1988).

[39] At large N, the quoted experimental values appear to converge to the value of an effective work function, W_{eff}, which is by ~0.8 eV systematically higher than the measured polycrystalline one ($W = 4.26$ eV), which was used in our calculations. Indeed, the low-temperature measurements for the IP's of Ag_N clusters given in Ref. [7] converge to $W = 4.26$ eV.

[40] In other instances, e.g., the widths of collective plasma excitations, shape fluctuations may play a larger role (see Ref. [33]).

[41] This ratio reduces the shell structure in the free energy by a factor larger than 10; shell-structure effects in the IP's and MSE's result from differences between two adjacent ΔF_{sh}'s and decrease even faster.

[42] Ref. [34], Vol. I.

[43] C. Bréchignac *et al.,* Phys. Rev. Lett. **77**, 251 (1996).